Volume 1 | Number 1 | Jan 2013 | Pages 1–100

Organic &
Biomolecular
Chemistry

www.rsc.org/obc

ROYAL SOCIETY
OF CHEMISTRY

ROYAL SOCIETY
OF CHEMISTRY

www.rsc.org/obc

Journal Name

ARTICLE

Developing a Targeting System for Bacterial Membranes: Measuring Receptor-Phosphatidylglycerol Interactions with ^{1}H NMR, ITC and Fluorescence Correlation Spectroscopy

Amanda Alliband, Zifan Wang, Christopher Thacker,† Douglas S. English* and Dennis H. Burns*

An ammonium picket porphyrin that targets bacterial membranes has been prepared and shown to bind to phosphatidylglycerol (PG), a bacterial lipid, when the lipid was in solution, contained within synthetic membrane vesicles, or when in Gram-negative and Gram-positive bacterial membranes. The multifunctional receptor was designed to interact with both the phosphate anion portion and neutral glycerol portion of the lipid headgroup. The receptor's affinity and selectivity for binding to surfactant vesicles or lipid vesicles that contain PG within their membranes was directly measured using fluorescence correlation spectroscopy (FCS). FCS demonstrated that the picket porphyrin's binding pocket was complementary for the lipid headgroup, since simple Coulumbic interactions alone did not induce binding. ^{1}H NMR and isothermal titration calorimetry (ITC) were used to determine the receptor's binding stoichiometry, receptor-lipid complex structure, binding constant, and associated thermodynamic properties of complexation in solution. The lipid-receptor binding motif in solution was shown to mirror the binding motif of membrane-bound PG and receptor. Cell lysis assays with *E. coli* (Gram-negative) and *Bacillus thuringiensis* (Gram-positive) probed with UV/Visible spectrophotometry indicated that the receptor was able to penetrate either bacterial cell wall and to bind to the bacterial inner membrane.

Introduction

Over a fifteen year period starting from the late 1930's, the first clinical use of antibiotics (sulfonamide and penicillin era) caused the mortality rate from infections in the United States to fall by approximately 75%.[1] Over a half century later, antibiotics still remain the first line of defense against pathogenic bacteria. However, in this same period there has been an emergence of many strains of multidrug-resistant (MDR) bacteria. Besides the well-known cases of Gram-positive MRSA and VRSA (*S. aureus*), there is a threat of truly untreatable infections by MDR and pan-drug resistant (PDR) Gram-negative bacteria. Pathogenic strains of *Acinetobacter baumannii*, *Escherichia coli*, *Klebsiella pneumoniae*, and *Pseudomonas aeruginosa* are now resistant to some (MDR) or all (PDR) antibiotics commonly used to treat these Gram-negative

ARTICLE

bacteria, such as penicillins, cephalosporins, carbapenems, monobactams quinolones, aminoglycosides, tetracyclines and polymyxins.[2] Extensively drug-resistant strains (XDR) of *Mycobacterium tuberculosis* and carbapenem-resistant (CRE) strains of *Klebsiella pneumoniae* are up and coming threats with high mortality rates of those infected. The emerging crisis of bacterial antibiotic resistance is considered to be epidemic, and has resulted in the US Centers for Disease Control and Prevention to declare in 2013 an urgent need for the development of new families of antimicrobial therapeutics to use against these "nightmare bacteria."

Of course, higher organisms do control bacterial growth, as this need has existed since the development of multicellular organisms. An antibacterial mechanism common to innate immune functions of all higher organisms is the selective targeting of bacterial membranes by antimicrobial peptides (AMP).[3-10] Notably, the outer leaflet of prokaryotic cell inner membrane contains an abundant supply of the anionic lipid PG, while the outer leaflets of eukaryotic cell membranes are almost exclusively composed of zwitterionic phospholipids.[11] Cationic AMPs utilize this difference in lipid structure to bind to the prokaryotic membrane via Coulumbic interactions followed by membrane insertion, membrane disruption and eventual bacterial cell death.

We have prepared and characterized the lipid binding ability of several phosphatidylglycerol receptors.[12,13] Armed with an understanding of the structures of bacterial membrane components and the ability to develop selective binding agents, our intent is to link synthetic PG receptors with compounds that exhibit either bacterial membrane disrupting properties (AMP mimic)[14] or compounds able to inhibit bacterial membrane proteins involved in virulence mechanisms[15] to afford new families of antibiotics. Importantly, both type of potential antimicrobials require a targeting system that is able to differentiate between prokaryotic membranes and eukaryotic membranes for it to be used as a systemic therapeutic. A synthetic conjugate that contains a PG receptor with a complementary binding pocket for PG will provide more selectivity than one based purely on charge recognition. As such, it will bring its antimicrobial component to the bacterial membrane, keep it on the membrane, and thereby increase the conjugate's effective concentration and ability to successfully complete its intended purpose.

We have previously shown that urea-picket porphyrins will bind to PG with 1:1 binding stoichiometry in organic solutions. These initial solution studies clarified the structural requirements for a complementary lipid binding pocket with the determination that four conformationally rigid urea-pickets align properly to allow hydrogen bonding with both the phosphate anion portion and the neutral hydroxyl portion of the lipid headgroup.[12] We now report a major advance in the development of our targeting system for bacterial membranes with the demonstration that a similarly configured, water-soluble ammonium-picket porphyrin can selectively bind with high affinity to synthetic membranes that contain PG. The structure of the lipid-receptor complex in solution or at a membrane surface was shown to be quite similar. These findings prompted further experiments, which substantiated that the porphyrin receptor would bind to bacterial membranes, presumably via their PG lipids. We show that a tetrakis-ammonium-picket porphyrin binds to PG with 1:1 binding stoichiometry in organic solvent, and using ^{1}H NMR spectroscopy and isothermal titration calorimetry (ITC) we detail the binding motif and associated thermodynamic properties of complex formation. We found that the tetra-ammonium receptor exhibited a high binding affinity and selectivity for surfactant and lipid vesicles that contain PG by using fluorescence correlation spectroscopy. Using cell lysis assays and UV/Visible spectroscopy we prove that the ammonium-picket porphyrin can penetrate both Gram-positive and Gram-negative bacterial cell walls and bind to the bacterial inner membrane.

1a: R = NHCH$_2$CH$_2$OCH$_2$C$_6$H$_5$
1b: R = NH(CH$_2$CH$_2$O)$_3$CH$_2$CH$_3$

TBA distearoyl-phosphatidylglycerol,
R = C$_{17}$H$_{35}$

TBAPG
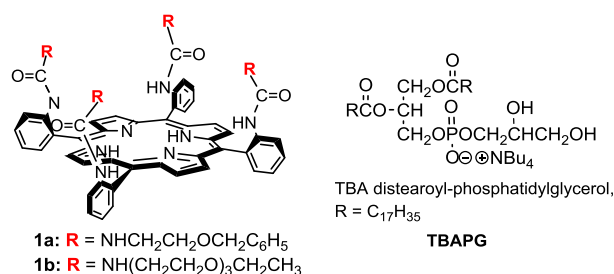
Figure 1. Structure of urea picket porphyrins and tetrabutylammonium phosphatidylglycerol.

Results and Discussion

Preparation and Solution Lipid Binding Ability of Ammonium-Picket Porphyrin. When the lipid receptor project was initiated we found no reported synthetic PG receptors, or no known PG-protein complex structure, to help guide the construction of PG binding pockets. A challenge in the preparation of a PG receptor's binding pocket is that it requires suitably spaced functionality to

bind and correctly align with two different sets of lipid functional groups, the phosphate anion portion and the neutral glycerol hydroxyl groups. The de novo design of our receptors was based entirely on modeling analysis, which demonstrated that the four pickets on the *meso*-phenyl rings of a porphyrin scaffold, appropriately functionalized, formed a complementary binding pocket to the lipid's multifunctional headgroup.[12] A synthetic advantage to the porphyrin structure is the inherent symmetry of the four pickets that are capable of alignment with the two different sets of lipid functional groups. Our initial studies showed that this was true for urea-picket porphyrins **1** when the pickets were relatively bulky and therefore conformationally rigid (only porphyrins with stable all-α atropisomers would bind to PG in a well-behaved 1:1 stoichiometry) (Figure 1). Desiring a water-soluble PG receptor to move beyond solution studies and allow for an investigation of the receptor's ability to interact with lipid membranes, we prepared a similarly structured tetrakis-ammoniumglycine-picket porphyrin. The relative straightforward synthesis of porphyrin **4a**[16] was accomplished by coupling the all-α atropisomer of 5,10,15,20-tetra(2-aminophenyl)porphyrin (**2**) with BOC-protected glycine to furnish porphyrin **3** followed by cleavage with TFA (Scheme 1). Although the glycine pickets were not bulky in structure it was hypothesized that the fully charged tetra-ammonium pickets would not readily form atropisomers due to destabilizing Coulombic interactions between the pickets. Variable temperature ^{1}H NMR experiments confirmed our hypothesis, establishing that no atropisomers occurred up to 100 °C. Complete counter-ion

exchange of TFA with PF$_6$ was accomplished by consecutive treatments of porphyrin **4a** with NH$_4$PF$_6$ (^{19}F and ^{31}P NMR spectra demonstrating the cleavage of the t-BOC groups and the complete exchange of the salt counterions are shown in S-Figures 6,10,11). The counterion exchange was done to make the charged receptor **4b** more soluble in organic solution and to help promote its crystallization for X-ray crystal analysis. Unfortunately, we were unable to prepare X-ray quality crystals of **4a** or **4b**.

Binding stoichiometry for the receptor-PG complex was established by Job plot analysis using ^{1}H NMR spectroscopy.[17,18] The solvent system of 60% CDCl$_3$/ 40% DMSO-d$_6$ provided sharp proton resonances in the NMR spectra of porphyrin **4b** and the receptor-lipid complex. In this solvent system the receptor-lipid binding stoichiometry was determined to be 1:1 (S-Figure 20). Not surprisingly, titration of **4b** with its four ammonium pickets using dihydrogenphosphate anion exhibited greater than 1:1 anion:receptor binding stoichiometry, making a direct comparison of binding constants between the two anions of little use.[19] On the other hand, stacked plots of both anion titrations showed that the glycine-picket's ammonium proton resonances found at 7.9 ppm (in both salts) initially moved downfield and then were lost in the baseline upon titration with PG or when the porphyrin was titrated with dihydrogen phosphate anion (S-Figures 14-17). The similar movements of the ammonium protons during both anion titrations indicated that the receptor was hydrogen bonding with both the phosphate anion portion of the lipid head group and the inorganic phosphate anion. Additionally, the glycine picket's methylene proton resonances at 2.84 ppm moved upfield when titrated with PG or inorganic phosphate anion. Presumably binding to the stronger phosphate anion (as opposed to PF$_6^-$) helped to stabilize the positively charged ammonium group and allowed for increased diamagnetic shielding of the glycine methylene protons. Binding isotherms were established from ^{1}H NMR titration experiments of the receptor **4b** with TBAPG and binding constants determined from non-linear regression analysis using EQNMR.[20] The average value of the binding constants taken from three titration experiments (each of which used an average determined from the movement of 2 proton resonances) was 4,900 M^{-1} (Table 1).
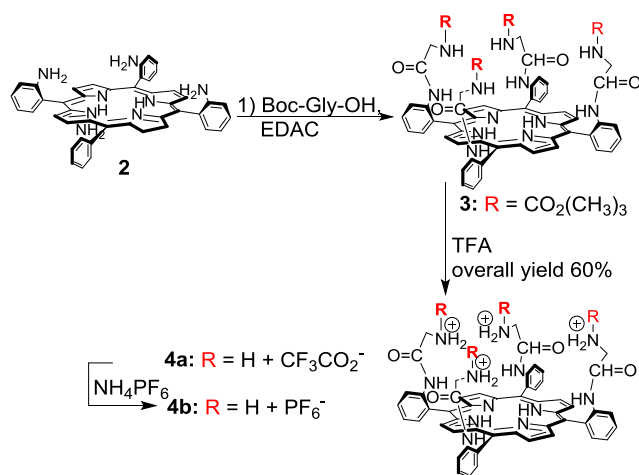
Scheme 1. Synthetic pathway for porphyrin **4**.

Table 1. Associated thermodynamic properties of receptor **4b** – PG complex formation.

Method	K_a (M^{-1})	ΔH kcal/ mol	ΔS cal/deg/mol
^{1}H NMR (30 ^{o}C)	4.9 x 10^3 (±5.4x10^2)	NA	NA
ITC (40 ^{o}C)	2.8 x 10^3 (±1.0 x 10^3)	0.7 (±0.09)	18

Solvent for NMR: 60% CDCl$_3$/ 40% DMSO-d$_6$; solvent for ITC: 50% DMSO/ 45% CHCl$_3$/ 5% CH$_3$OH.

Upon reverse titration of the lipid with **4b** the glycerol protons (multiplets between 3.35-3.85 ppm[12]) moved upfield during complex formation, indicating the glycerol headgroup lies directly above the ring (S-Figure 19). In this orientation one would expect PG headgroup protons to shift upfield due to the positioning of these protons within the porphyrin's large, shielding ring current. ^{1}H NMR spectroscopy confirmed that ammonium receptor **4b** orients the lipid headgroup in such a way that at least one of its hydroxyl groups would be positioned to hydrogen bond with one of the receptor's ammonium or amide hydrogens, concomitantly while the phosphate anion portion is bound to one or perhaps in between two ammonium pickets.[12] Previously we have shown that inorganic phosphate anion will bind its anionic oxygen between two urea pickets via hydrogen bonds with similarly structured urea picket porphyrins.[19]

The receptor's amide proton resonance at 9.15 ppm moves downfield and broadens into the baseline upon PG titration. It is possible that this is due to the picket's amide proton hydrogen bonding with the hydroxyl groups on PG. Or, since the amide proton lies just above the porphyrin ring, the shift in proton resonance could be caused by changes to the macrocyclic ring current upon binding the anion. It has been our experience with urea picket porphyrins that upon binding an anion the β-protons shift upfield by 0.2 ppm or more due to a reduction in ring current.[17,19,21] In this case, the upfield β-proton shift is less than 0.02 ppm, demonstrating that the ring current is little changed. The above described receptor-PG complex structure would cause a displacement of DMSO solvent that is hydrogen bonded to the amide within the binding pocket.[17,19,21] Loss of solvent would lead to an expected upfield shift in the amide proton unless the PG replaced lost solvent with one of its hydroxyl groups as a hydrogen-bonding acceptor. In point of fact, the receptor's amide protons do move upfield upon titration with dihydrogenphosphate anion. This suggests that with complex formation solvent is removed from the

binding pocket. In this case, however, there would be little possibility of the small inorganic anion hydrogen-bonding to the amide protons when also bound to an ammonium group, resulting in the observed upfield shift.

The associated enthalpy and entropy of receptor **4b**-lipid complex formation was determined by isothermal titration calorimetry (ITC, Table 1). To obtain well-behaved, repeatable results required a change in solvent system used in NMR titrations to the ternary system of 50% DMSO/ 45% CHCl$_3$/ 5% CH$_3$OH. The control addition of TBAPG alone to the solvent system was slightly exothermic, while the addition of the PG to the receptor solution was slightly endothermic (see S-Figure 21). The small enthalpy changes upon titration of receptor with PG necessitated the ternary solvent system whose use produced the smallest experimental perturbations observed in the ITC data. Unlike the urea picket porphyrins **1** with which receptor-lipid complex formation was both enthalpy- and entropy-driven,[12] receptor-lipid binding with the ammonium picket porphyrin **4b** was only entropy driven (18 cal/deg/mol), which is expected in a charged system.[22] Even with the use of a different solvent system, the ITC's average binding constant of 2,800 M^{-1} was similar to the binding constant determined by NMR titrations.

The ^{1}H NMR spectrum of **4b** (S-Figure 8) shows that the ammonium protons integrate to the correct number of 12 protons (the ammonium protons overlay 4 aromatic protons at approximately 7.9 ppm), and the ESI HRMS (S-Figure 13) clearly shows molecular ions corresponding to (M+H)$^+$, (M+PF$_6$+2H)$^+$, (M+2PF$_6$+3H)$^+$, and (M+3PF$_6$+4H)$^+$. The fluorine and phosphorus NMR spectra are correct for the PF$_6$ counterion present in receptor **4b**. The ^{1}H NMR spectrum of **4a** (S-Figure 4) also indicates that there are 12 ammonium protons (the ammonium protons overlay 8 aromatic protons at approximately 7.9 ppm) but the ESI HRMS only showed a (M+2H)$^{+2}$/2 molecular ion (S-Figure 7). Upon drying **4a** under vacuum in a drying pistol at 112 ^{o}C for 24-48 hrs the receptor would not only lose water molecules but also molecules of TFA. As such (and without an X-ray crystal structure of the charged porphyrin), a sample of receptor **4b** was placed in a vial and subjected to a stream of nitrogen overnight and sent for elemental analysis to determine the weight percent ratio of nitrogen to fluorine (under these conditions water and ethyl acetate remained bound to the receptor, but these solvent impurities would not affect the F:N weight percent ratio). The elemental analysis determined the weight percent ratio of F:N to be 1.0: 0.646, which is consistent with the MF =

$C_{60}F_{12}H_{50}N_{12}O_{12} \cdot 0.5$ TFA. The proton, fluorine, and phosphorus NMR spectra, the ESI HRMS and the EA data taken all together indicate that the receptor's four amino pickets are fully charged.

Fluorescence Correlation Spectroscopy (FCS): A Direct Probe for Receptor-Membrane Binding. As the TFA-porphyrin salt **4a** was more soluble in aqueous solution than the PF_6-porphyrin salt **4b**, the TFA-porphyrin salt was used in the synthetic membrane experiments. FCS was used to provide a spectroscopic probe for receptor binding to PG-doped vesicle membranes. FCS is a microscope-based technique using laser-induced fluorescence that provides a reliable, fast and accurate method for determining binding of biomolecules to vesicle bilayers[23-26] and even absolute numbers of fluorophores bound to a larger construct.[27] The vesicles provide a bio-mimetic platform for evaluating receptor affinity and selectivity when PG is part of the bilayer. In our experiments the receptor was directly excited and its fluorescence emission collected and evaluated by autocorrelation analysis, since the porphyrin acted as its own fluorophore. Autocorrelation analysis provides a quantitative, and visual, indication of the degree of binding due to changes that appear in the autocorrelation function's decay time caused by the *apparent* change in the receptor diffusion rate when the small receptor (~ 1 nm) binds to the larger vesicle (>100 nm).[27] *These experiments directly probe the association of receptor with the PG headgroup at the surface of a bilayer membrane.*

Three types of vesicles were used in the experiments and these were vesicles formed from phosphatidylethanolamine (PE) that included either PG or phosphatidylserine (PS) (where 30% PG/70% PE was used as a model for an *E. coli* membrane;[28] PS is an anionic lipid found in the inner leaflet of animal cell membranes) and vesicles formed from mixtures of the single-tailed surfactants cetyltrimethylammonium tosylate (CTAT) and sodium dodecylbenzenesulfonate (SDBS) that were doped with PG. In all experiments, pre-formed vesicles were added to receptor solutions. In all cases the concentration of receptor and total concentration of vesicle components were held constant with the vesicle containing varying percentages of PG or PS.

The fluctuations of fluorescence intensity were processed by standard autocorrelation analysis according to equation 1:

$$G(\tau) = \frac{<\delta F(t)\delta F(t+\tau)>}{<F(t)>^2} \quad \text{(eq. 1)}$$

The autocorrelation decays were fit with the function in equation 2:

$$G(\tau) = (f + \frac{A}{N}e^{-\frac{\tau}{\tau_{triplet}}}) \bullet f \bullet C_1 \bullet \frac{1}{\left(1+\frac{\tau}{\tau_D}\right)} \bullet \frac{1}{\left(1+\left(\frac{r_0}{z_0}\right)^2\left(\frac{\tau}{\tau_D}\right)\right)^{1/2}}$$

$$+ (1 - f + (1-f)Ae^{-\frac{\tau}{\tau_{triplet}}}) \bullet C_2 \bullet \frac{1}{\left(1+\frac{\tau}{\tau'_D}\right)} \bullet \frac{1}{\left(1+\left(\frac{r_0}{z_0}\right)^2\left(\frac{\tau}{\tau'_D}\right)\right)^{1/2}}$$

(eq. 2)

where f is the fraction of receptor that is bound to vesicles. The diffusion times for vesicle-bound receptors and free receptor are τ_D and τ'_D, respectively. The triplet relaxation time of the receptor is $\tau_{triplet}$ (1.8 µs). The detection volume is defined by r_0 and z_0 that correspond to the $1/e^2$ lengths of the radial and axial axes of the three dimensional observation volume. N is the average number of receptors in the observation volume. The quantity A is proportional to the ratio of intersystem crossing rates between the singlet and triplet manifolds. The coefficients C_1 and C_2 are inverse proportionality constants for the number of vesicles and receptors present in the observation volume. Specifically $C_1 = \frac{G_0}{(V_{obs} \times [\text{Vesicle}])}$ where V_{obs} is the observation volume defined by the focused laser beam and [Vesicle] is the vesicle concentration. Similarly, $C_2 = \frac{G_0}{(V_{obs} \times [\text{receptor}])} = \frac{G_0}{N}$. The quantity G_o is a scaling factor determined from the autocorrelation decay of free receptor in the absence of vesicles. When fitting the autocorrelation decays, C_1 is kept fixed and C_2 varies as G_o/N. Separate experiments were conducted in which the radial and axial spatial parameters were determined independently using the autocorrelation decay obtained from carboxylate-modified fluorescent microspheres with diameters of 0.1 and 0.02 µm (Fluorosphere, Invitrogen). In the receptor binding experiments, the autocorrelation decays were fit to two variables, f and N.
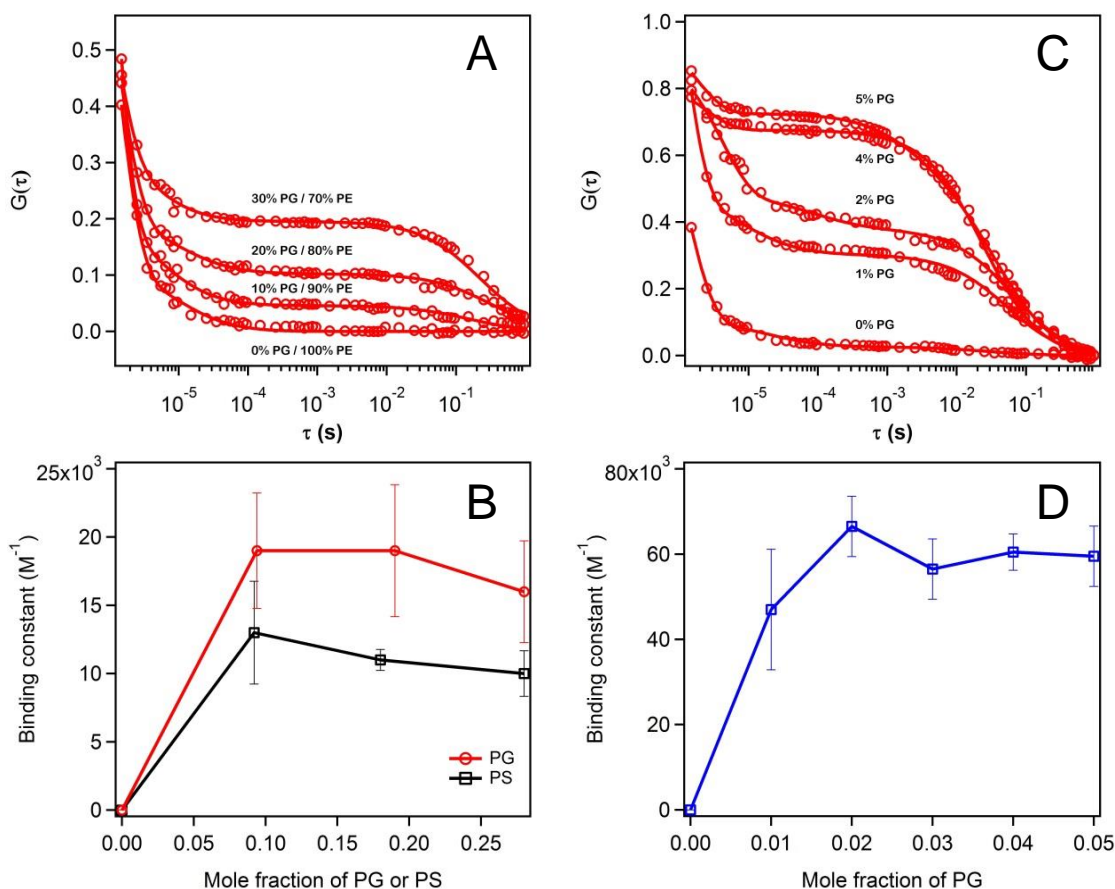
Figure 2. Autocorrelation analysis of receptor binding to PG-doped membranes of liposomes and positively-charged surfactant vesicles. In panels A and C, the open circles are experimental data and the solid line is a fit to equation 2. A) Autocorrelation decays for receptor with varying percentages of PG in PE liposome. B) Binding constant values as a function of PS and PG in PE liposome. C) Autocorrelation decays for receptor with varying percentages of PG in positively-charged surfactant vesicles. D) Binding constant of receptor with varying percentages of PG in positively-charged surfactant vesicles.

Organic & Biomolecular Chemistry

Figure 2 shows the results of the experiments for both types of vesicles. The autocorrelation decays were acquired from receptor with various mole fractions of PG or PS present in the different vesicle membranes. The relative amplitudes of the fast and slow decay components changed with the amount of PG in the membrane. In each case, as the fraction of PG was increased, the contribution from the fast, microsecond-range component decreased. This was due to the removal of rapidly-diffusing, unbound receptor and also from the decrease in the contribution from triplet dynamics of receptor that was bound to the vesicle. In panels A and C of Figure 2, the autocorrelation decays of the receptor in the absence of PG is rapid (~10 μs) and is dominated by intersystem crossing, i.e. blinking. The amplitude of long component is proportional to $f^2/$ [V] and therefore this amplitude increased as more PG was introduced. The fraction bound (f) was determined by fitting the autocorrelation decay and was used to find the binding constant as shown in equation 3:

$$K = \frac{[\text{bound receptor}]}{[\text{free receptor}][\text{free PG}]} = \frac{f}{(1-f)(\frac{[\text{PG}]}{2}-[\text{R}]f)}$$

(eq. 3)

where [R] is total concentration of receptor and it has been assumed that half of the PG is located on the membrane outer leaflet.

Figure 2A shows the autocorrelation decays acquired from varying amounts of PG in PE vesicles doped with PG. This data, along with data from PE vesicles doped with PS (not shown), was used to find the binding constants that are plotted in Panel 2B and given in Table 3. No binding was observed for pure PE vesicles. When either PG or PS was present receptor binding constants on the order of 10^4 were measured and the binding constant for PG was found to be roughly twice that of PS, showing a modest level of selectivity. The data presented in Table 3 shows that the binding constants vary little whether the vesicle contained 10%, 20%, or 30% PG within its lipid membrane, and the receptor fraction bound increases proportionally to the increase in PG % within experimental error. The result indicates that there is no (positive or negative) cooperativity in receptor-membrane binding, and the receptor-lipid binding stoichiometry is effectively 1:1. This strongly suggests there is proper alignment of receptor and lipid functional groups within the complex formed at the membrane surface just as is found in the receptor-lipid complex in solution.

Autocorrelation decays for the receptor in solutions containing surfactant vesicles doped with PG are shown in Figure 2C. The overall positively charged vesicles were formed from the spontaneous self-assembly of a mixture containing a 1.8:1 molar ratio of cationic surfactant (CTAT) to anionic components (SDBS and PG) thus resulting in a bilayer with a constant anion percentage (36%) but with variable amounts of PG. Negligible binding of the receptor was observed when the synthetic vesicle contained no PG and the only anionic component was SDBS. When the vesicle contained as little as 1% of PG and 35% SDBS the binding constant increased from negligible to 4.7 x 10^4 (Table 4). This dramatic increase in binding to the membrane surface is another indication that the receptor's binding pocket was complementary for the membrane-bound lipid. The results show that receptor-lipid interactions were chemically specific since simple Coulombic interactions alone were not enough to induce binding (the total percent of anionic character within the vesicles did not change). As shown in Panels 2C and 2D, binding was observed at very low doping levels and surprisingly the calculated binding constants were three-fold higher than those measured in the overall negatively charged PG/PE vesicles. The larger binding constants may be due to better accessibility of the PG headgroup in the surfactant bilayer due to tail-group length mismatch. Whatever the reasons, it is noteworthy that the four-plus charged receptor was able to bind to the overall cationic vesicle at all. The receptor's K_a for membrane-bound lipid in aqueous solution is roughly 3-4 times greater than for binding lipid in organic solvent. While noting that the two systems are quite different, one can speculate that the entropic contribution to membrane binding is larger due to more solvent molecules released upon complex formation, as membrane lipid headgroups are highly hydrated. Additionally, the k_{off}'s contribution to the K_a may be decreased because, when the receptor is bound at the membrane surface, it may be more difficult to re-solvate the binding pocket compared to a complex that is fully solvated in solution.

Table 3. Binding constants for receptor **4a** determined by FCS for lipid vesicles.

Vesicles consisting of various PG percentages with PE				
% PG in vesicle	0%	10%	20%	30%
Receptor fraction bound, f	0	0.06 ± 0.01	0.10 ± 0.03	0.13 ± 0.03
K_a (M^{-1}) x 10^4	0	1.9 ± 0.4	1.9 ± 0.5	1.6 ± 0.4
Vesicles consisting of various PS percentages with PE				
% PS in vesicle	0%	10%	20%	30%
Receptor fraction bound, f	0	0.05 ± 0.01	0.06 ± 0.01	0.08 ± 0.02
K_a (M^{-1}) x 10^4	0	1.3 ± 0.4	1.1 ± 0.1	1.0 ± 0.2

Table 4. Binding constants for receptor **4a** with differing amounts of PG in surfactant vesicle while keeping the same overall anionic concentration.

Vesicles consisting of PG, SDBS and CTAT (1.8:1 ratio of + to -)						
% PG in vesicle	0%	1%	2%	3%	4%	5%
Receptor fraction bound, f	3x10^{-3}± 8x10^{-4}	0.09± 0.02	0.20± 0.02	0.23± 0.03	0.31± 0.02	0.36± 0.04
K_a (M^{-1}) x 10^4	Minute	4.7± 1.4	6.9± 0.7	5.4± 0.7	6.1± 0.4	6.2± 0.7

Experiments to Determine Ability of Receptor to Pass through Bacterial Cell Wall and Bind to Bacterial Membrane. To be useful as the targeting component of an antimicrobial therapeutic the receptor must be able to pass through the bacterial cell wall and ultimately bind to the membrane-bound PG. Having demonstrated the ability of the porphyrin receptor to selectively bind to synthetic membrane vesicles which contain PG, we turned to experiments to determine whether the receptor could pass through the bacterial outer layers of the cell wall and bind to the cytoplasmic membrane. Fortunately, the large extinction coefficient of macrocycle's **4a** Soret band made this determination fairly straightforward via UV/Visible spectroscopy.

An aqueous solution of receptor was used to furnish either a 10μM or 25μM receptor concentration of bacterial solutions comprised of 1 mL 25mM HEPES/0.9% NaCl buffer (see Experimental for details). Both *E. coli* (Gram-negative) and *Bacillus thuringiensis* (Gram-positive) were used in these experiments. The bacteria were incubated with the receptor for 1, 2 or 4 hr duration.

After the appropriate time period the bacterial broth was centrifuged and the supernatant was removed for spectral analysis. The pellet was suspended in 1 mL 0.9% NaCl, and the cells were collected and repeatedly washed by centrifugation, while each time the supernatant of the wash was removed for spectral analysis. After the third wash the bacterial cells were suspended in 1 mL HEPES/NaCl buffer (25mM/0.9%) and the cells were lysed by sonication, the bacterial components centrifuged, and the supernatant was removed for spectral analysis. Finally, this pellet was resuspended with 1 mL CelLytic B detergent to dissolve membrane-bound components, and then the solution was centrifuged and the supernatant removed for spectral analysis. The first supernatant contained receptor that did not enter the bacterial cell and was still dissolved in the buffer solution, while the supernatants from the wash presumably contained receptor that may have been weakly bound to the outside of the bacterial cell wall. Both the lipid A and small amount of PG in Gram-negative bacterial walls, or the teichoic acids in the Gram-positive walls (anionic due to attached phosphate residues), could interact with the positively charged receptor. The supernatant from the sonication lysate contained receptor that had passed through the bacterial cell wall, but which was not bound to a membrane component (i.e., anything large enough to sediment). Finally, the detergent supernatant contained receptor removed from the dissolved membrane components to which they were tightly bound.
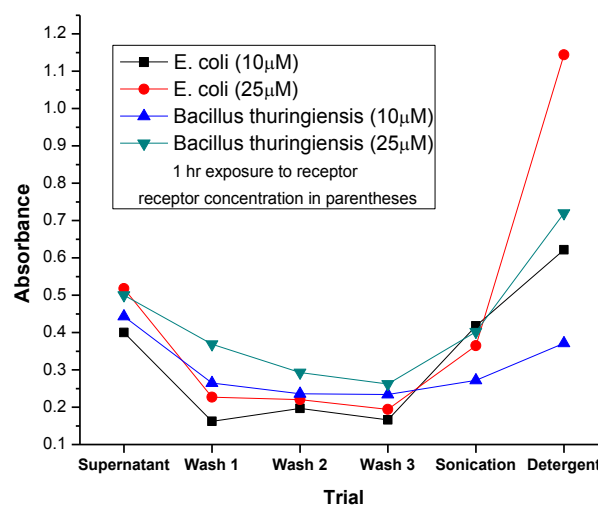

Figure 3. Absorbance (420 nm) of supernatants of various trials with *E. coli and Bacillus thuringiensis* after incubating the bacterial solutions with receptor (10 or 25 μM) for 1 hr.

The following results are the average from two sets of experiments with each bacterium. Figure 3 shows the absorbance (Soret band maximum at 420 nm) results of the supernatants described above for the 1 hr incubation using both the 10μM and 25μM receptor **4a** concentrations with *E. coli* and *Bacillus thuringiensis* (see S-Figure 22 for 2 and 4 hr incubation data). The experimental results are qualitative but informative, and demonstrate three salient points. First, the receptor clearly passes through both the Gram-negative wall of *E. coli* and the Gram-positive wall of *Bacillus thuringiensis*. Secondly, the majority of receptor passed through both bacteria's cell wall in all but the 1 hr - 10μM *Bacillus thuringiensis* experiment. Thirdly, the largest percentage of internal receptor was bound to membrane components. It is noteworthy that the observed difference in absorbance between the supernatants afforded after sonication and then with addition of detergent increase as the time of bacteria exposure to receptor increases from 1 hr to 4 hr. Given the demonstrated ability of receptor **4a** to bind to PG contained in synthetic lipids, it is likely that most of the receptor which passed through the cell wall was able to bind to the inner membrane via its PG lipids, increasingly so as incubation time was doubled and then quadrupled, and was only removed when lipid membranes were dissolved in a detergent solution. It is unclear at this time if the difference in uptake of receptor between the two bacteria observed in the above experiments was due to the difference in cell wall structure, a difference in the percent of PG in the inner membrane, or both.

Conclusions

Our results have proved that it is possible to design a receptor that exhibits high affinity and selectivity for vesicle-bound PG at the membrane surface utilizing a receptor-lipid binding motif first elucidated by solution studies. The structure of the porphyrin-lipid complex in organic solution as determined from ^{1}H NMR is one where the anionic phosphate and neutral hydroxyl groups of PG align and interact with the multifunctional groups in the binding pocket formed from the pickets of the receptor. As previously reported with our urea picket receptors, the 1:1 receptor-lipid binding stoichiometry implies full alignment of interacting functional groups in the receptor-lipid complex.[12] Without proper alignment, functional groups that are not involved in receptor-lipid interactions are then free to bind to a third partner resulting in complex binding stoichiometry.

FCS was shown to be a powerful aid in the development of our lipid receptor, affording 1) rapid determination of receptor-membrane binding, 2) the use of extremely small sample size and 3) binding analysis on a receptor-lipid complex formed at an actual membrane interface. Surfactant vesicles doped with PG as probed by FCS demonstrated that the receptor selectively targets membrane-bound PG based on multifunctional binding pocket complementarity rather than just Coulombic interaction. When using lipid vesicles FCS proved quite capable of determining the receptor's binding strength for membrane-bound PG. FCS provided evidence that the binding motif at the membrane surface is similar to the receptor-lipid binding motif in solution, i.e., at the membrane surface there is proper alignment of the PG lipid's headgroup and receptor functionality. The bacteria experiments demonstrated that the receptor could penetrate the bacterial cell wall, and provided evidence that binding to synthetic lipid membranes was a good indication that the receptor could bind to actual bacterial inner membranes as well. *Thus, results from the solution experiments, synthetic membrane experiments and the bacteria experiments all corroborate one another*. All results were supportive of the initial hypothesis that the picket porphyrin's binding pocket would exhibit complementarity for its lipid guest, with the multifunctional groups in both receptor and PG appropriately aligned.

The modest selectivity of the receptor for PG over PS as ascertained by FCS is most likely due to the simplicity in the picket structures, with the charges at their termini. It is likely that extending the pickets above the ammonium groups would increase the selectivity for PG over PS due to different steric and electronic requirements of a binding pocket for an ammonium/carboxylate headgroup rather than a neutral glycerol headgroup. Additionally, extended pickets could provide membrane insertion units which would increase membrane binding affinity (in previous work we demonstrated that the section of picket above the urea groups in porphyrins **1a** and **1b** affected the amount of associated entropy of receptor-lipid complex formation in solution[12]). We are currently modifying the ammonium pickets to determine if these hypotheses have merit and working on ways to modify the picket porphyrin for straightforward attachments to membrane disrupting groups.

Experimental Section

^{1}H NMR Titrations. ^{1}H NMR titrations to determine association constants were done as described in reference 11. In this

case, the NMR solvents were 60% CDCl$_3$/ 40% DMSO-d$_6$, the temperature was 30 ^{o}C and the movements of the proton resonances were averaged from a minimum of three titration experiments and each experiment's value was averaged using two proton resonances (glycine methylene protons and porphyrin β-protons). Non-linear regression analysis using EQNMR furnished the receptor-lipid association constants.

Job plots. The receptor was dried in a vacuum desiccator over P$_2$O$_5$ and the lipid dried in a vacuum desiccator over drierite. The lipid and receptor were weighed on a microbalance and each placed into a 2 ml volumetric flask; the amounts used allowed for identical molar concentrations. Aliquots of receptor solution and lipid solution (60% CDCl$_3$/ 40% DMSO-d$_6$) were placed into separate NMR tubes, such that 1 tube contained 1 equivalent of receptor and 0 equivalent of lipid; the next tube contained 0.9 equivalents of receptor and 0.1 equivalents of lipid; the next tube contained 0.8 equivalents of receptor and 0.2 equivalents of lipid, and so forth down to 0.1 equivalents of receptor and 0.9 equivalents of lipid. In this way, the sum of the molar equivalents of both anion and receptor was always the same. Once the solutions had been added to the tube they were diluted with 60% CDCl$_3$/ 40% DMSO-d$_6$ so that the volume in each tube was 0.45 ml. A spectrum was then obtained for each tube, and the change in chemical shift of receptor proton resonances relative to the shift recorded from the tube with no added lipid was determined. The mole fraction of receptor was plotted vs. the change in chemical shift multiplied by the mole fraction of receptor in the tube to afford the Job plots. Job experiments were done at slightly different concentrations to remove any artifacts caused by different concentrations when using ^{1}H NMR.

Isothermal Titration Calorimetry. ITC experiments were done with a MicroCal iTC200 to determine the enthalpy of association. All data analysis was done with Origin software supplied by MicroCal, using a model for the stoichiometry of binding that was determined from the Job plots. Control titrations were performed by the addition of lipid solution to a solution of 50% DMSO/ 45% CHCl$_3$/ 5% CH$_3$OH and these control titrations were subtracted from the titrations of lipid to receptor to remove the effects of heats of dilution. All ITC experiments were run at 40 ^{o}C. The results are averaged from a minimum of three ITC experiments, and all experiments were done at slightly different concentrations to

detect problems associated with possible impurities such as from crystalline solvent, etc.

Synthetic Vesicle Preparation. Synthetic vesicle samples prepared from aqueous mixtures of CTAT and SDBS were doped with varying amounts of PG. Methods for doping these types of vesicles have been described previously and were followed here.[31,32] Initial samples were prepared with a total surfactant concentration of 1% by weight. CTAT-rich vesicle preparations were 7:3 CTAT: SDBS by weight (0.07 g CTAT and 0.03 g SDBS). Positively-charged vesicles containing PG, SDBS and CTAT were prepared by substituting SDBS with PG to keep the charge-ratio of the bilayer components uniform in all samples. The ratio of cation to anion was 1.8:1. The vesicles were prepared by dissolving a mixture of dry surfactants and PG in a HEPES buffer solution (25 mM) containing Na$_2$SO$_4$ (50 mM). A pH of 6.5 was obtained by addition of NaOH. The synthetic vesicle solutions were stirred for 72 hours to ensure surfactants had dissolved and equilibrium had been reached.

Liposome Preparation. Two types of liposomes were prepared – liposomes containing PE and PG with PG mole fractions 0, 0.094, 0.19, 0.28 and liposomes containing PE and PS with PS mole fractions 0, 0.092, 0.18, 0.28. The lipid mixtures were dissolved in CHCl$_3$: MeOH: H$_2$O (65:35:8 by volume). The solvent was removed under reduced pressure. The resulting films were hydrated with 10 mL of the HEPES solution described above for an initial concentration of 3.5 mg/mL. The solution was stirred and heated to 85 °C under a nitrogen gas atmosphere until the sample is fully hydrated. Unilamellar vesicles were formed by extruding 4 times with a mini-extruder (Avanti Polar Lipids, Alabaster, AL) and polycarbonate membranes with 200 nm pore size (Whatman-GE Healthcare Life Sciences, Pittsburgh, PA).

Fluorescence Correlation Spectroscopy. The binding of receptor to vesicles as a function of PG mole ratio in liposomes and synthetic vesicles was studied using preformed vesicles, followed by dilution and receptor addition before performing FCS experiments. FCS was performed at room temperature with an instrument consisting of an air cooled argon ion laser (532-AP-A01, Melles Griot, Carlsbad, CA), an inverted microscope (Axiovert 200, Carl Zeiss, Göttingen, Germany) and a single photon counting avalanche photodiode (SPCM-AQR-15, Perkin Elmer, Vaudreuil, QC, Canada). The circularly polarized excitation beam (λ= 514 nm) was delivered by a single mode optical fiber and focused into the sample

solution approximately 10 μm from the coverslip surface using a 100X, 1.30 N.A. oil immersion objective (Fluar, Carl Zeiss). This resulted in a nearly diffraction limited spot with a lateral radius of r_0~310 nm and axial axes of z_0~1500 nm. The laser power was maintained at 10 μW. The emitted fluorescence (625-750 nm) was collected by the same objective and separated from excitation light via a dichroic mirror (Chroma Technology Corp, Bellows Falls, VT) and a long pass filter (λ=514.4 nm, Semrock, Rochester, NY). The fluorescence was refocused onto a 50 μm pinhole (Throlabs, Newton, NJ) to eliminate background fluorescence originating outside of the focal volume. Output of the photodiode was fed to a counter timer board (PCI-6602, National Instruments, Austin, TX) operating in time-tagged photon counting mode using home written software in LabVIEW (National Instruments, Austin, TX.). In time-tagged mode, each detected photon is assigned a number corresponding to the elapsed time from the previous detection event. These "time-tags" were then used to construct the autocorrelation curve. Temporal resolution for timed tagged data is limited by the on-board clock of the counter/timer board (80 MHz) which leads to a time interval of 12.5 ns. The time tagged data was auto correlated off-line using routines written with Igor Pro 6.22.

α,α,α,α-5,10,15,20-tetrakis-(2-(*N*-[(2-t-butylcarbamoyl)ethanamide]phenyl)-porphyrin (3): Under a nitrogen gas atmosphere, dry porphyrin **2** (0.3235 g, 0.479 mmol, 1 equiv.) and BOC-Gly-OH (0.3779 g, 2.157 mmol, 4.5 equiv.) in dry CH_2Cl_2 (8.7 mL) and transferred to an ice bath. EDAC·HCl (0.3676 g, 1.918 mmol, 4 equiv.) in dry CH_2Cl_2 (6.5 mL) was added to the reaction mixture and it was allowed to stir overnight in an ice bath. The solution was washed with water (2 x 25 mL) and the organic layer was dried with Na_2SO_4. The solution was filtered and concentrated under reduced pressure. The product was purified using column chromatography eluting with $EtOAc:CH_2Cl_2$ (1:1) to yield a purple solid (0.3196 g, 0.2452 mmol, 62%). Mp: 186 – 188°C; UV/Vis DMF λ max (lnε): 423.0 (12.72), 516.0 (10.07), 549.0 (9.18), 590.0 (9.13), 655.0 (8.72); ^{1}H NMR (400 MHz, DMSO) δ 8.82 (s, broad, 4H), 8.69 (s, 8H), 8.14 (d, 4H, J = 8.4 Hz), 7.93 (d, 4H, J = 6.8 Hz), 7.84 (t, 4H, J = 7.8 Hz), 7.58 (t, 4H, J = 7.8 Hz), 6.44 (s, broad, 4H), 2.83 (s, 8H), 1.001 (s, 36H), -2.77 (s, 2H); ^{13}C NMR (100 MHz, DMSO) δ 168.2, 155.4, 137.9, 136.0, 134.5, 131.1, 129.2, 124.7, 124.0, 115.6, 77.9, 42.9, 27.8; HRMS (ESI) calcd for $C_{72}H_{78}N_{12}O_{12}$ (M+H)$^+$ 1303.5940, found 1303.6008; HRMS (ESI) cald for $C_{72}H_{78}N_{12}O_{12}Na$ (M+Na)$^+$ 1325.5760, found 1325.5718.

α,α,α,α-5,10,15,20-tetrakis-(2-(*N*-[(2-ammonium)ethanamide]phenyl)porphyrin tetrakistrifluoroacetate (4a): Porphyrin **3** (0.6233 g, 0.478 mmol, 1 equiv.) was dissolved in CH_2Cl_2 (11.8 mL) and transferred to an ice bath. TFA (11.8 mL) was added to the solution and the reaction mixture was allowed to stir overnight in an ice bath. The reaction mixture was concentrated under reduced pressure. Diethyl ether was triturated to remove excess TFA and removed under reduced pressure to yield a purple solid which was dried with a drying pistol (0.797 g, 0.586 mmol, 62%). Mp: 201 – 203°C; UV/Vis DMF λ max (lnε): 428.5 (11.29), 521.0 (9.32), 553.5 (8.12), 593.5 (8.19), 659.0 (7.81); ^{1}H NMR (400 MHz, DMSO) δ 9.63 (s, broad, 4H), 8.64 (s, 8H), 8.27 (d, 4H, J = 8.4 Hz), 7.80-8.00 (m, 20 H), 7.58 (t, 4 H, J = 7.4 Hz), 2.85 (s, 8H), -2.74 (s, 2H); ^{13}C NMR (100 MHz, DMSO) δ 165.3, 158.3, 137.4, 135.8, 134.2, 130.8, 129.3, 124.3, 124.2, 117.7, 115.3, 114.8, 76.7; ^{19}F (376 MHz, DMSO, calibrated to CF_3CO_2H: -75.52 ppm) δ -76.55 (s, 12F); ESI HRMS calcd for $C_{52}H_{48}N_{12}O_4$ (M+2H)$^{+2}$/2 452.1961, found 452.1940.

α,α,α,α-5,10,15,20-tetrakis-(2-(*N*-[(2-ammonium)ethanamide]phenyl)porphyrin tetrakishexafluorophosphate: Ammonium hexafluorophosphate (1.108 g, 6.80 mmol, 20 equiv.) was dissolved in EtOAc (37.8 mL) and added to the porphyrin **4a** (0.4393 g, 0.340 mmol, 1 equiv.) in EtOAc. The reaction mixture was allowed to stir overnight at rt. Water (17 mL) was added to the reaction mixture and allowed to stir for 30 min. The layers were separated and the organic layer was washed water (2 x 17 mL). The combined organic layers were dried with Na_2SO_4, filtered and concentrated under reduced pressure. To the product (0.4067 g) was added ammonium hexafluorophosphate (1.026 g, 6.29 mmol, 20 equiv.) in EtOAc (35 mL). The reaction mixture was allowed to stir at rt overnight. Water (15.8 mL) was added to the reaction mixture and it was allowed to stir for 30 min. The layers were separated and the organic layer was washed with water (2 x 15.8 mL). The combined organic layers was dried with Na_2SO_4, filtered and concentrated under reduced pressure to yield a purple solid (0.2184 g, 0.1469 mmol, 51%). Mp: 270°C, dec; UV/Vis DMF λ max (lnε): 421.0 (16.47), 517.0 (13.63), 549.0 (12.40), 591.0 (12.46), 651.0 (12.11); ^{1}H NMR (400 MHz, DMSO) δ 9.66 (s, broad, 4H), 8.73 (s, 8H), 8.26 (d, 4H, J = 8 Hz), 7.92 (t, 8H, J = 7.8 Hz), 7.78 (s, broad, 12H), 7.55-7.65 (m, 4H), 2.96 (s, 8H), -2.74 (s, 2H); ^{13}C NMR (100 MHz, DMSO) δ 165.5, 136.76, 136.67, 134.4, 131.3, 129.4, 124.84, 124.63, 115.7, 40.5; ^{19}F (376 MHz, DMSO, calibrated to CF_3CO_2H: -75.52 ppm) δ -71.55 (d, 24F, J =

711 Hz); ^{31}P (161 MHz, DMSO, calibrated to 75% H_3PO_4 0.00 ppm) δ 106.23 (septet, 4P, J = 707 Hz); HRMS (ESI) calcd for $C_{52}H_{47}N_{12}O_4$ (M+H)$^+$ 903.3843, found 903.3878; calcd for $C_{52}F_6H_{48}N_{12}O_4P$ (M+PF$_6$+2H)$^+$ 1049.3563, found 1049.3684; calcd for $C_{52}F_{12}H_{49}N_{12}O_4P_2$ (M+2PF$_6$+3H)$^+$ 1195.3283, found 1195.3276; calcd for $C_{52}F_{18}H_{50}N_{12}O_4P_3$ (M+3PF$_6$+4H)$^+$ 1341.3003, found 1341.3066.

Bacterial Cell Lysis Experiments: A plate of the bacteria was streaked out and incubated for 24 hours at 37 °C. Using aseptic technique, a single colony of bacteria was selected and added to 5mL of autoclaved LB growth media. This was shaken and incubated at 37 °C overnight. This 5mL culture was then transferred to 100mL of autoclaved LB growth media to produce a 100mL culture. This culture was then shaken and incubated for 3 hours to achieve an optical density of 600. It was then divided into two 50 mL centrifuge tubes and both were centrifuged in a large centrifuge at 3,000 rpm for 10 minutes. The supernatant (LB Growth Media) of each was removed, and both bacterial pellets were re-suspended in 50mL of 0.9% NaCl solution. These were again centrifuged and the washing procedure was repeated. After the second NaCl wash supernatant had been removed, the pellets were each re-suspended in 5mL of 25 mM HEPES/0.9% NaCl buffer. Solutions were homogenized and then seven 1 mL aliquots were taken and added to 1.5mL Eppendorf tubes. A 500 μM solution of the receptor dissolved in pure water was freshly made. Then the appropriate amount was added to the Eppendorf tubes (either 0.05 mL or 0.02 mL) to reach the desired receptor concentration. The Eppendorf tubes were then closed and periodically shaken to mix the solution.

The following procedure is the same for all Eppendorf tubes used in the lysis experiments. When the set time for the incubation of the bacterial solution with receptor was complete, the Eppendorf tube was spun down in a micro-centrifuge. The supernatant was removed and collected for analysis. The bacterial pellet was re-suspended in 1 mL 0.9% NaCl wash, and this solution was homogenized and then centrifuged. The supernatant wash was removed and collected and the process repeated two more times. After the third wash was complete, the pellet was re-suspended in 1 mL 25 mM HEPES/0.9% NaCl buffer solution. The Eppendorf tube was then placed onto crushed ice to cool for a couple of minutes before sonication. The solution was then sonicated at regular intervals over a one minute time period to lyse the bacterial cells. This mixture was allowed to cool and then centrifuged. At this point

the bacterial pellet was fairly purple due to the coloration of the porphyrin. Buffer was removed and collected, and then 1 mL CelLytic B detergent was added to the pellet to break down membrane components that came from the bacterial cells. The mixture was homogenized, and after centrifugation, the detergent supernatant was collected. All of the collected supernatant samples were diluted by a factor of two and then analyzed using UV-Vis spectroscopy.

Acknowledgements

Notes and references

Electronic Supplementary Information (ESI) available: HRMS, ^{1}H NMR and ^{13}C NMR spectra of **3**, **4a**, **4b**, ^{19}F NMR spectra of **4a** and **4b**, ^{31}P NMR of **4b**, stacked ^{1}H NMR plots of **4b** titrated with TBAPG or TBAH$_2$PO$_4$, ^{1}H NMR of **4b** + CD$_3$OD, stacked ^{1}H NMR plots of TBAPG titrated with **4b**, Job plot and binding isotherm of TBAPG and receptor **4b**, ITC binding isotherms of receptor **4b** with TBAPG, cell lysis assay results of bacteria incubated with receptor **4a** for 2 or 4 hr, partial UV/Visible and Fluorescence spectra of porphyrin **4a**. See DOI: 10.1039/b000000x/

† NIH/ KINBRE undergraduate scholar

1. B. Spellberg, "The Antibacterial Pipeline: Why Is It Drying Up, and What Must Be Done About It" IOM. 2010. *Antibiotic Resistance: Implications for Global Health and Novel Intervention Strategies*. Washington, DC: The National Academic Press.
2. M. Fischbach, C. T. Walsh, "Antibiotics for Emerging Pathogens" IOM. 2010. *Antibiotic Resistance: Implications for Global Health and Novel Intervention Strategies*. Washington, DC: The National Academic Press.
3. A. T. Y. Yeung, S. L. Gellatly, R. E. Hancock, *Cell. Mol. Life Sci.* **2011**, *68*, 2161-2176.
4. R. F. Epand, J. E. Pollard, J. O. Wright, P. B. Savage, R. M. Epand, *Antimicrob. Agents Chemother.* **2010**, *54*, 3708-3713.
5. A. Giuliani, A. C. Rinaldi, *Cell. Mol. Life Sci.* **2011**, *68*, 2255-2266.
6. V. Lazarev, V. Govorum, *Appl. Biochem. Microbiol.* **2010**, *46*, 803-814.
7. P. Oyston, M. Fox, S. Richards, G. J.Clark, *Med. Microbiol.* **2009**, *58*, 977-987.
8. H. Jenssen, *PharmaChem: Peptides* **2009**, *8*, 22-26.
9. G. N. Tew, R. W. Scott, M. L. Klein, W. F. Degrado, *Acc. Chem. Res.* **2010**, *43*, 30-39.
10. R. E. Hancock, D. S. Chapple, *Antimicrob. Agents Chemother.* **1999** *43* 1317-1323.
11. I. Kustanovich, D. Shalev, M. Mikhlin, L. Gaidukov, A. J. Mor, *Biol. Chem.* **2002**, *277*, 16941-16951.
12. A. Alliband, F. A. Meece, C. Jayasinghe, D. H. Burns, *J. Org. Chem.* **2013**, *78*, 356-362.
13. M. B. Koralegedara, H. W. Aw, D. H. Burns, *J. Org. Chem.*, **2011**, 76, 1930-1933.
14. X.-Z. Lai, Y. Feng, J. Pollard, J. N. Chin, M. J. Rybak, R. Bucki,

R. F. Epand, R. M. Epand, P. B. Savage, *Acc. Chem. Res.* **2008,** *41*, 1233-1240.

15. Y. Gotoh, Y. Eguchi, T. Watanabe, S. Okamoto, A. Doi, R. Utsumi, *Curr. Opin. Microbiol.* **2010** *13*, 232-239.

16. M. Ushiyama, Y. Katayama, T. Yamamura, *Chem. Lett.* **1995**, 395-396.

17. D. H. Burns, K. Calderon-Kawasaki, S. Kularatne, *J. Org. Chem.* **2005**, *70*, 2803-2807.

18. Dilution studies with the TBAPG salt and the receptor were conducted in 60% $CDCl_3$/ 40% DMSO-d_6 to determine the appropriate concentrations for receptor and anion salts in the ^1H NMR stoichiometric studies.

19. K. Calderon-Kawasaki, S. Kularatne, Y. H. Li, B. C. Noll, W. R. Scheidt, D. H. Burns, *J. Org. Chem.* **2007,** *72***,** 9081-9087.

20. Binding constants were determined by non-linear regression analysis using EQNMR for Windows: M. J. Hynes, *J. Chem. Soc. Dalton Trans.* **1993**, 311-312.

21. R. C. Jagessar, M. Shang, W. R. Scheidt, D. H. Burns, *J. Am. Chem. Soc.,* **1998**, *120*, 11684-11692.

22. F. P. Schmidtchen, *Coord. Chem. Rev.* **2006**, *250* 2918-2928.

23. S. B. Lioi, X. Wang, M. R. Islam, E. J. Danoff, D. S. English, *Phys. Chem. Chem. Phys.* **2009,** *11*, 9315 - 9325.

24. L. Rusu, A. Gambhir, S. McLaughlin, J. Radler, *Biophys J* **2004,** *87* (2), 1044-1053.

25. M. A. Morgan, K. Okamoto, J. D. Kahn, D. S. English, *Biophys. J.* **2005,** *89* (4), 2588-2596.

26. D. Magde, E. L. Elson, W. W. Webb, *Biopolymers* **1974,** *13* (1), 29-61.

27. Y. D. Yin, R. F. Yuan, X. S. Zhao, *J. Phys. Chem. Lett.* **2013,** *4* (2), 304-309.

28. A. Malina, Y. Shai, *Biochem. J.* **2005**, *390*, 695-702.

29. N. Fatin-Rouge, K. J. Wilkinson, J. Buffle, *J Phys Chem B* **2006,** *110* (41), 20133-20142.

30. E. Haustein, P. Schwille, *Methods* **2003,** *29* (2), 153-166.

31. S. A. Walker, J. A. Zasadzinski, *Langmuir* **1997**, *13*, 5076-5081.

32. G. B. Thomas, L. H. Rader, J. Park, L. Abezgauz, D. Danino, P. DeShong, D. S. English, *J. Am. Chem. Soc.* **2009**, 131, 5471-5477.

Organic & Biomolecular Chemistry Accepted Manuscript